Signal Processing for Acoustic Emission Signature Analysis and Defect Detection

Yeldos A. Altay
Department of Robotics and Technical Means of Automation
Satbayev University
Almaty, Kazakhstan
aeldos@inbox.ru

Dmitry O. Kuzivanov
Faculty of Control Systems and Robotics
ITMO University
Saint-Petersburg, Russian Federation
kuzivanovdmitry@gmail.com

Dinara A. Altay
Military Engineering Institute of Radio Electronics and Communications
Department of Natural Sciences
Almaty, Kazakhstan
dinara.altai@mail.ru

Alexey V. Fedorov
Faculty of Control Systems and Robotics
ITMO University
Saint-Petersburg, Russian Federation
avfedorov@itmo.ru

2024 26th International Conference on Digital Signal Processing and its Applications (DSPA) | 979-8-3503-6172-8/24/$31.00 ©2024 IEEE | DOI: 10.1109/DSPA60853.2024.10510110

Abstract— **This article presents the results of implementing a digital signal processing method for analyzing the acoustic emission (AE) signature and detecting defects such as cracks and pores. The signal processing method is based on a cascade connection of digital high-pass filters and ensures the selection of informative signals and increases the signal-to-interference ratio. In order to control the formation of defects in the process of selective laser melting, the paper presents the results of experimental testing of the cascade filtration method for detecting defects in the internal structure such as cracks and pores. The signal components recorded during the development of defects during the growth of additive manufacturing products were extracted. AE signatures were analyzed and statistical relationships were assessed. The relationship between the parameters of the AE signal and the values of laser radiation power has been identified, which characterizes the process of defect formation.**

Keywords- digital filter, high-pass filter, Butterworth filter, signal-to-noise ratio, defect, acoustic emission, pores, cracks.

I. INTRODUCTION

In non-destructive testing for diagnostics and technical condition control of products acoustic control methods, namely acoustic emission (AE), are widely used [1],[2]. Methods of non-destructive acoustic testing without destroying the integrity of products, the service life and suitability of the test object make it possible to identify, diagnose and control their technical condition. The method of AE is based on the physical phenomena of the acoustoelastic effect during the rearrangement materials structure of the test object. When using the AE method, the technical condition of the test object is accessed based on the interpretation recorded AE data. Recording of this data, as a rule, is carried out on the basis of specialized piezoelectric and electromagnetic transducers fixed on the surface of the tested object using a contact waveguide of a conductive substance [1]-[5]. The AE method has become widespread for solving problems of pipeline control, leaks [6], dynamically loaded rolling stock elements [1] and for diagnosing fatigue cracks [7],[8] defect formation processes [9], as well as for studying the deformation process [10],[11] which proves the applicability of this method to control the technical condition of products.

However, the AE signal is inevitably affected by interference of various types and characteristics, which reduces the accuracy of the obtained processing results [12]. Improving the accuracy of processing these signals is carried out by using special signal processing methods that are resistant to interference. The AE signal is affected by interference that occurs during the operation of power electrical installations, inducing electrical impulses into the measuring path, during welding, during machining and milling of the test object, from the loading device, during cavitation, during the outflow of liquid [12]. Among these interferences, the attenuation of the electrical noise of the pulsed form is a non-trivial task [13]. This is due to the fact that the interference has not only the sum deterministic components, but also the variability in the amplitudes values as non-stationary signals [13]-[15]. The effect of this interference reduces the accuracy of measuring information components and makes it impossible to correctly interpret AE events.

In additive technologies, the AE method is applicable for evaluating manufactured complex-shaped products based on selective laser melting (SLM) technology [16],[17]. SLM technology is used in engine building, shipbuilding, power and transport engineering, aircraft building and medicine [18]. In SLM, AE signals are affected by low-frequency and high-frequency noise. Low-frequency noises arise due to mechanical

Authorized licensed use limited to: Satbayev University. Downloaded on April 03,2026 at 09:50:27 UTC from IEEE Xplore. Restrictions apply.

vibrations SLM equipment [16]. High-frequency noise is generated by laser emitting and the operation servo drive of the SLM equipment, which induce noise in the form of an electrical impulse and continuous noise. The presence of noise in AE signals significantly reduces their measurement accuracy and diagnostic parameters, as well as the signal-to-noise ratio (SNR) [19]. Compensation for the influence of these noises can be carried out on the basis of digital filtering methods. During the noise digital filtering an important task is to save the waveform AE that carries diagnostic information [14]. For filtering these noise a review of scientific papers published in the e-Library, Scopus, Springer Nature, Google Scholar databases with a 20-year retrospective period was carried out. This review of filtering methods has shown that polynomial digital filtering methods based on Butterworth filter are less consecrated for AE signal processing. Considering this, the method of polynomial digital filtering are investigated, justified and proposed in the works [13],[15],[20] for processing the recording of full-scale AE signals.

This method provides stable filtering of natural AE signals with the required values of filter quality indicators (transition time, overshoot, gain) [13], which is confirmed by the placement of root loci (zeros and poles) inside the unit circle on the right side of the complex plane. The choice of this method is justified by the possibility of carrying out high-precision filtering with minimal distortion of the informative component of the AE signal shape [19], as well as resistance to the distorting effect of interference [20].

In this paper presents the results of AE monitoring of the process of pore formation and cracking in products during their SLM process based on the use of processing of recorded noisy AE signals using the polynomial cascade filtering method. The work also provides a statistical assessment of the influence of various SLM modes on the formation of defects.

In this article, unlike the published scientific works [13]-[15], [19],[20] the results of full-scale AE signals processing based on cascade high-frequency filtering method for AE signature analysis and defect detection.

II. Filter Synthesis, Tuning and Scheme

A. Filter Synthesis

The synthesis of a polynomial digital high-pass filter is based on the use mathematical apparatus of transfer functions. Polynomial digital high-pass filter, namely the Butterworth is infinite impulse response. Its synthesis is carried out in a normalized range, namely normalized filter analog low frequencies, i.e. with a cutoff frequency ω=1 rad/*s*. The transfer function of such a filter is defined as follow [13]:

$$W_{norm}(s) = \frac{\omega_c^m}{A(s)} = \frac{1}{A(s)} \quad (1)$$

where s – complex variable, ω_c – cut of frequency, m – filter order, $A(s)$ – filter polynomial. The Butterworth polynomial coefficients $A(s)$ in the denominator of transfer function of this filter are found from the expression

$$A(s) = s^m + a_1\omega_c s^{m-1} + \ldots + a_{m-1}\omega_c^{m-1}s + \omega_c^m = \sum_{i=1}^{m}(s - s_i^*),$$

where a - polynomial coefficients, $s_i^* = \omega_c \sqrt[2m]{(-1)^{m+1}}, i = \overline{1,m}.$

In order to avoid the introduced distorting effect of high-order filters on the signal parameters and reduce the cumbersomeness of calculating the transfer function of the filters, the choice of a second-order polynomial (m=2) is justified. The transfer function of continuous high-pass with cutoff frequency ω_c is found from the transfer function low-pass filter of the normalized form (1) by replacing the operator s with the operator for high frequencies $\frac{\omega_c}{s}$. The transfer function synthesized high-pass filter $W(s)$ presented below.

$$W(s) = W_{norm}(s)\Big|_{s\to\frac{\omega_C}{s}} = \frac{1}{\left(\frac{\omega_c}{s}\right)^2 + 1.414\frac{\omega_c}{s} + 1} =$$

$$= \frac{1}{\frac{s^2 + 1.414\omega_c s + \omega_c^2}{s^2}} = \frac{s^2}{s^2 + 1.414\omega_c s + \omega_c^2}$$

The minimal waveform distortion is achieved by using a bi-directional processing method based on a synthesized high-pass filter. During such processing, noisy signals are filtered in the forward and then in the reverse direction [13]. The resulting distortions introduced by the filtering system are mutually compensated.

B. Filter Tuning

Considering the sources of noise arising during SLM [16], their identification was carried out. For this identification, before melting, the AE equipment was simultaneously started with the SLM equipment turned on, and noise signals were recorded when the manipulator was moved. As a result, a signal of a mixture from continuous noise and an electrical impulse was recorded. Based on the discrete Fourier transform, the noise signal frequency was estimated to justify the cutoff frequency tuned high-pass Butterworth IIR filter second order. The discrete Fourier transform is an efficient signal analysis method for identifying unknown frequency components of a signal and noise [13], [21]. In Fig. 3 shows the noise signal spectrum and the frequency spectrum.

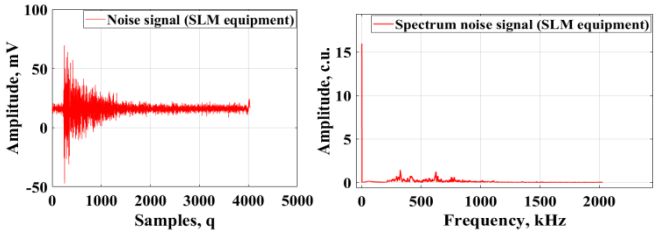


Fig. 1. The acoustical noise signal amplitude-time (right) and the amplitude-frequency (bottom) spectrum.

The identification results showed that the frequencies of full-scale SLM noise signal are in the frequency range from

Authorized licensed use limited to: Satbayev University. Downloaded on April 03,2026 at 09:50:27 UTC from IEEE Xplore. Restrictions apply.

300 kHz to 1000 kHz. According to studies [22]-[24] the frequency of AE signals from vaporization is below the level of 100 kHz. This makes it possible to justify the choice of the lower (up to 100 kHz) and upper (up to 250 kHz) boundaries of the frequency range for tuning two frequencies in order to isolate the signal of AE cracking, pore formation and interference suppression, frequencies localized on the spectrum above 250 kHz.

The filter parameters were tuned by normalizing and transforming the noise cutoff frequency. This type of tuning of filter parameters allows saving a continuous signal frequency during digital signal processing [13]. For this, it is initially necessary to determine the cutoff frequency ω_C in the normalized frequency range. The normalized cutoff frequency refers to the absolute frequency normalized to the sampling rate. After normalizing the cutoff frequency, the frequency scale was transformed for the relationship of frequency characteristics between continuous ω_C and discrete cutoff frequencies of the Ω_C filter. This approach is equivalent to the assumption that the sampling interval is T=1s, which makes it possible to simplify the mathematical calculations during the analysis and tuning of the digital filter.

Normalization and transformation of the filter cutoff frequency were determined in the following form [13]:

$$\begin{cases} \omega_C = \left(\frac{f_C}{f_D}\right)\cdot 2\pi, \\ \Omega_C = \left(\frac{2}{T}\right) tg\left(\frac{\omega_C}{2}\right) \end{cases}$$

The transformation transfer function $W_1(s)$ and $W_2(s)$ into a digital transfer function W_1 (z) and W_2 (z) was carried out by a bilinear transformation in the MATLAB program using the function bilinear(), as $s = \frac{2}{T}\left(\frac{1-z^{-1}}{1+z^{-1}}\right)$ at T=1s.

$$\begin{cases} W_1(s) = \dfrac{s^2}{s^2 + 0{,}06364s + 0{,}002025} \\ W_2(s) = \dfrac{s^2}{s^2 + 0{,}1768s + 0{,}01563} \end{cases}$$

$$\begin{cases} W_1(z) = \dfrac{0{,}9687z^2 - 1{,}937z + 0{,}9687}{z^2 - 1{,}936z + 0{,}9384} \\ W_2(z) = \dfrac{0{,}9155z^2 - 1{,}831z + 0{,}9155}{z^2 - 1{,}824z + 0{,}8382} \end{cases}$$

The analysis of the quality indicators showed that digital HF filters frequencies tuned to a cutoff frequency of 100 and 250 kHz are stable, their gain coefficient at cutoff frequencies is 0.7. The roots-poles and roots-zeros of the calculated filters are localized at pole locuses $p_{1,2} = 0.968 \pm 0.0308i$ for fc = 100 kHz and $p_{1,2} = 0.912 \pm 0.080i$ for fc = 250 kHz, as well as at zero loci at z=0.999≈ 1. The analysis confirms the localization of the roots of the high frequency transfer function inside the unit circle, namely on the right side of the complex z plane, and the filters are considered stable for cascading filtering of full-scale AE signals.

C. Cascade Filtering Scheme

Cascading bi-directional filtering is implemented in the MATLAB software product version R2017b according to the block diagram shown in Fig. 2.

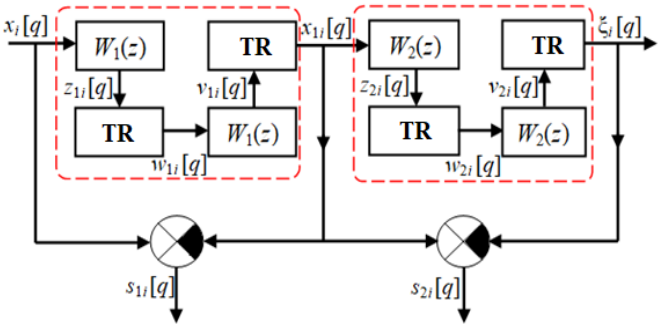


Fig. 2. Block diagram of processing for isolating AE signals from pore formation and cracking.

According to the developed block diagram, with bi-directional filtering, the input sequence of noisy signals i AE is processed by filters $z_{1i}[q]$ and $z_{2i}[q]$ of the first and second sequences in the forward direction, then using the time reverse block (TR), the sequence of counts $w_{1i}[q]$ and $w_{2i}[q]$ of filtered signals is reversed. The received samples of the i AE signals are processed in the opposite direction $v_{1i}[q]$ and $v_{2i}[q]$ using $W_1(z)$ and $W_2(z)$, then the final time inversion at the output of the TR block leads to a change in the order of the samples to the reverse. At the output of the TR block, filters mutually compensate the introduced distortions and the corresponding signals are generated.

The addition of the **adder-subtractor** block ensures the formation of signals from defects of a specific type, for example, the $s_{1i}[q]$ signal characterizes the process of porosity formation and $s_{2i}[q]$ cracking. The signals $\xi_i[q]$ are only high-frequency interference affecting the characteristics of the AE parameters. The separation of AE signals into $s_{1i}[q]$ and $s_{2i}[q]$ also makes it possible to quantify the ratio of these informative signals to interference $\xi_i[q]$ similar to [17] the signal-to-noise ratio (SNR). The indicators evaluated in this way characterize an increase in the quality of signal processing at the output of each sequence of the filter cascade.

III. Signal-to-Noise Ratio Assessments

The results of cascade filtering showed that the average value of the SNR at the output of the high frequency increases, which confirms the distinguishability of the values of this indicator and an increase in the effectiveness of signal processing [25]. The result of the assessment of the SNR indicator is presented in Fig. 3 in the form of a Tukey diagram illustrating the improvement in the effectiveness of AE signal processing.

Authorized licensed use limited to: Satbayev University. Downloaded on April 03,2026 at 09:50:27 UTC from IEEE Xplore. Restrictions apply.

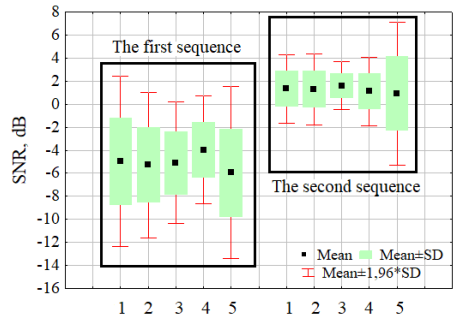


Fig. 3. SNR indicator evaluation Tukey diagram

At the same time, the distinguishability of the values of the experimental SNR indicator at the output of each HF filter is confirmed by the statistics of the T-test (Table. 1; M - mean, SD - standard deviation, *p* - statistical significance), where the AE control data from defects are presented in groups (the first and second sequence).

TABLE I. TABLE TYPE STYLES

Sample	M±SD, dB		
	The first sequence	*The second sequence*	*p-value*
1	-4.957±3.779	1.335±1.519	0.034
2	-5.267±3.222	1.298±1.574	0.015
3	-5.093±2.699	1.593±1.058	0.013
4	-3.959±2.396	1.119±1.518	0.007
5	-5.949±3.808	0.938±3.168	0.001
Note: the indicators are statistically significant at $p < 0.05$			

The average SNR value for each sample, calculated at the output of the first sequence of the filter cascade, differs statistically significantly from the average value of the SNR of the second sequence. It should be noted that the negative SNR indicator at the output of the first sequence of the filter cascade is due to the lower amplitude of the selected AE signal relative to the amplitude of the interference.

It was noted in [26] that the negative or low value of the indicator characterizing the attenuation of interference at the output of the filter cascade for low-amplitude signals of complex shape and structure is due to the fact that the amplitude of the measured AE signals [10] is lower than the amplitude of the interference [8]. This also confirms the correctness of the assessment of this indicator.

IV. AE SIGNAL PROCESSING AND SIGNATURE ANALYSIS

This section presents the results of AE signal processing the based on bi-directional implementation of the high-pass cascade filters (100 kHz and 250 kHz). In order to better visualize filtered full-scale AE signal results, Fig. 4 shows noise signal processing and porosity and crack signal extraction.

A. AE Signal Processing

The results of the analysis showed that AE signals from pores (Fig. 4) and cracks (Fig. 5) differ in shape and characteristics from each other, as well as from a noisy signal (Fig. 3). At the same time, the maximum amplitude of the signals on sample number 5 is much higher than on number 1.

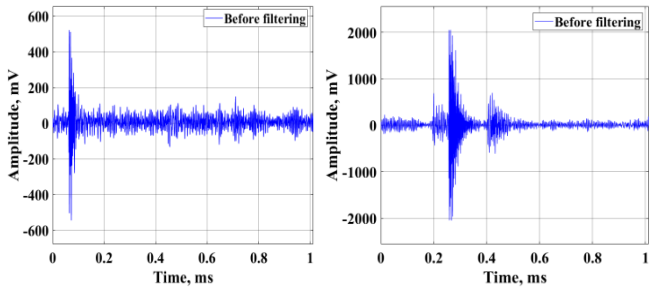


Fig. 4. AE signals before filtering results for sample number 1 (left) and sample number 5 (right).

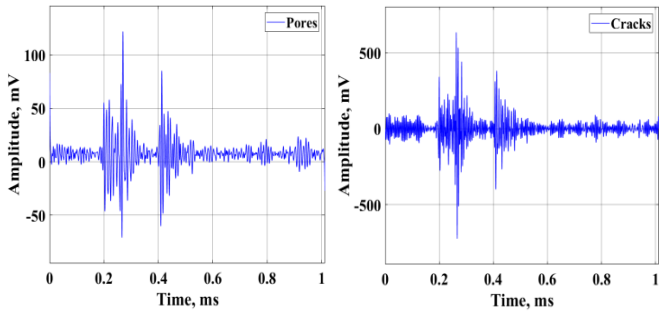


Fig. 5. AE signals from pore formation for sample number 1 (left) and sample number 5 (right).

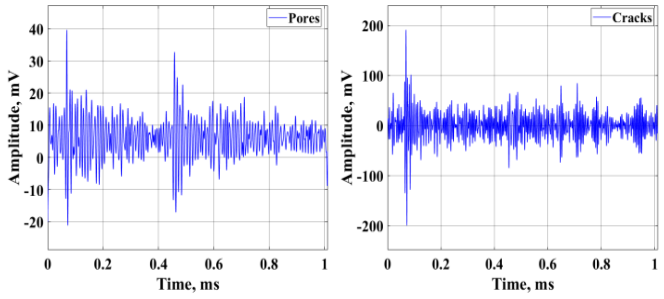


Fig. 6. AE signals from crack formation for sample number 1 (left) and sample number 5 (right).

B. Signature Analysis

The analysis of AE signatures was carried out on the basis of T-test statistics, which allows us to evaluate the measurement results between channels and samples.

TABLE II. CHARACTERISTICS OF AE AMPLITUDE BY CHANNEL

Sample	M±SD, mV			
	Before filtering	*Pore formation*	*Cracking*	*Noise*
1	2402.000±1217.335 *p*=0.029*	632.068±46 7.251 *p*=0.073*	418.181±292.325 *p* = 0.064*	155.288±69 5.665 *p* = 0.020*
	p = 0.019**		*p* = 0.024**	*p* = 0.048**

Authorized licensed use limited to: Satbayev University. Downloaded on April 03,2026 at 09:50:27 UTC from IEEE Xplore. Restrictions apply.

Sample	M±SD, mV			
	Before filtering	*Pore formation*	*Cracking*	*Noise*
2	1712.500±706.873 $p = 0.016$*	467.817±132.935 $p = 0.005$*	422.652±93.120 $p = 0.002$*	993.767±453.865 $p = 0.022$*
	$p = 0.024$**		$p = 0.026$**	$p = 0.011$**
3	2000.750±794.011 $p = 0.015$*	492.749±216.329 $p = 0.019$*	428.969±504.904 $p = 0.013$*	106.367±440.299 $p = 0.016$*
	$p = 0.013$**		$p = 0.015$**	$p = 0.013$**
4	2205.750±995.030 $p = 0.021$*	600.711±101.621 $p = 0.001$*	504.904±116.576 $p = 0.003$*	131.271±586.070 $p = 0.020$*
	$p = 0.045$**		$p = 0.046$**	$p = 0.022$**
5	2433.500±1492.962 $p = 0.047$*	872.869±914.056 $p = 0.012$*	646.229±688.105 $p = 0.015$*	164.222±107.397 $p = 0.055$*
	$p = 0.032$**		$p = 0.036$**	$p = 0.032$**

Note:
* – the difference in average amplitude values between channels;
**– the difference in amplitude before and after the implementation of the filtration method.

From the Table 2 it can be seen that the average value of the measured AE signals of each channel during the control of each sample is statistically significantly different from the average value of the signals in the other group. The difference in the average values of noisy and filtered signals is due to the high efficiency of the digital filtering method.

The value of the AE amplitude increases from sample to sample, this is due to the restructuring of the internal structure of the material. Therefore, the discrete AE signal characterizes the crystallization process of the Inconel (EP648) alloy under the influence of laser radiation power at various stages of SLM.

Due to analysis of AE amplitude for each melting pass, it was found out that the average value of the AE amplitude and the total AE amplitude during the control of the passes of growing sample number 5 are higher (by 70% and 100%, respectively) than during the control sample number 1, which indicates the possible formation of defects in sample number 5 (Fig. 7).

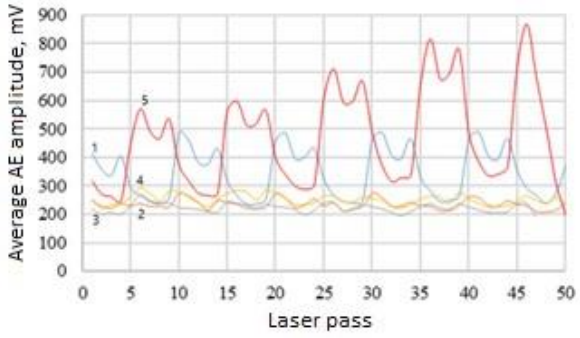


Fig. 7. AE signature analysis

It is known [27] that the presence of defects in the crystal cell (CC) or the destruction of internal structural bonds of products causes irreversible displacements of neighboring matrices bonds. At the same time, the strength and stability of structural bonds in the CC also largely depends on the nature of defects.

One of the main factors that significantly influence the quality of manufactured products is the laser radiation power. The statistical dependence describing the influence of laser radiation power on the amplitude of discrete AE is presented in Fig. 8.

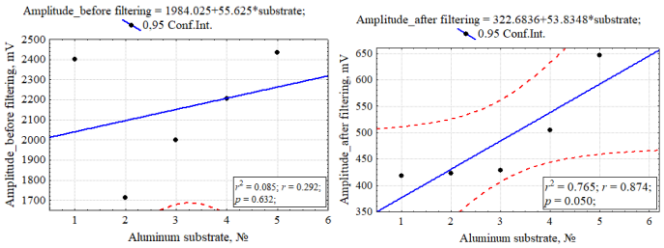


Fig. 8. Signal average amplitude scattergram before filtering (left) and after (right) filtering.

The scattergram shows that for the result before filtering there is a correlation $r = 0.2$ with a statistical significance coefficient $p = 0.632$. According to the Chaddock assessment scale [20], this correlation is considered negligible and not statistically significant. After filtering correlation coefficient, the value increases to r=0.874 with the statistical significance p=0.050. Regression analysis result confirmed the positive effect filtering method on increasing the information analysis of AE signal parameters. This effect can be confirmed by the coefficient of determination $r^2 = 0.765$ and characterized based on artificial intelligent method, namely linear regression. The linear regression method is a highly sensitive data training method that does not require special and specific training the acoustic control test data. The analyzed data can be characterized by the linear regression equation, as: $y_{\text{after filtering}} = 53.8348 \cdot \text{aluminum substrate} + 322.6836$ at $r^2 = 0.765$, $p = 0.050$, $r = 0.874$, respectively.

This article also evaluates the correlation between the amplitude of discrete AE from pore formation, cracking and interference. The results showed that there is also a non-random high correlation between the AE amplitudes during pore formation and cracking: r=0.896, r^2=0.804 at p=0.039. The presence of this relationship characterizes structural transformations in the material of the samples.

It seems important that there is no high statistically significant connection between the amplitudes of discrete AE from defects and the influencing interference. In [28] it is noted that in the frequency response of the AE transducer (AET) above 250 kHz to 400 kHz, resonant frequencies from the dominant frequency of 160 kHz are traced, where the frequency components of the interference that arise during the movement of the manipulator of the robotic installation of the AET in this work are located. No relationship between indicators $r_{\text{noise: pore formation}} = 0.211$ at $p = 0.435$ and $r_{\text{noise: cracking}} = 0.103$ at $p = 0.597$ between the amplitude of discrete AE and noise indicates that the frequency components of the

Authorized licensed use limited to: Satbayev University. Downloaded on April 03,2026 at 09:50:27 UTC from IEEE Xplore. Restrictions apply.

informative signals of discrete AE are distinguishable from the noise components, therefore, the process is not correlated.

V. CONCLUSION

This article presents the results of AE monitoring of defect formation in samples manufactured by the SLM method. To process AE testing data, it is proposed to use the cascade filtering method. The results of testing the method showed that:

- the value of the SNR indicator after filtering is on average higher than 1.5 dB, which characterizes the stability of AE signals to influencing interference;
- the value of the correlation coefficient between the laser radiation power and the amplitude of the discrete AE after filtering increases by 3 times, which characterizes the effectiveness of the processing.

REFERENCES

[1] Gomez M.P. Assessment of cutting tool condition by acoustic emission. Procedia materials science, 2012, V. 1, pp. 321-328.

[2] Mao W., Hei L., Yang Y. Advances on the acoustic emission testing for monitoring of granular soils. Measurement, 2021, V. 185, pp. 110110.

[3] Barile C., Casavola C., Pappalettera G., Kannan V.P. Application of different acoustic emission descriptors in damage assessment of fiber reinforced plastics: A comprehensive review. Engineering fracture mechanics, 2020, V. 235, pp. 107083.

[4] Bekher S.A., Muravev V.V., Muravev M.V. Novel techniques of AE signal processing for upgrading the accuracy of flaw localization. Russian journal of nondestructive testing, 2002, V. 38, pp. 600-610.

[5] Zhao L., Kang L., Yao S. Research and application of acoustic emission signal processing technology. IEEE Access, 2019, V. 7, pp. 984-993

[6] Bekher S.A., Sych T.V. Development of methodology for the calculation and experimental investigation of acoustic emission signals. AIP conference proceedings, 2017, V. 1915, p. 020001.

[7] Barat V., Terentyev D., Bardakov V., Elizarov S. Analytical modeling of acoustic emission signals in thin-walled objects. Applied sciences, 2019, V.10, pp. 279.

[8] Barat V., Bardakov V. Features of noise filtering during acoustic emission testing. International Journal of innovative technology and exploring engineering, 2019, V. 9, pp. 3977-3980.

[9] Stepanova K.A., Kinzhagulov I.Y., Kovalevich A.S., Alifanova I.E., Ashikhin D.S., Yakovlev Y.O. Applying laser-ultrasonic and acoustic emission methods to nondestrictive testing at different stages of deformation formation in friction stir welding. Russian journal of nondestructive testing, 2020, V. 56, pp. 191-200.

[10] Agletdinov E., Merson D., Vinogradov A. A new method of low amplitude signal detection and its application in acoustic emission. Applied sciences, 2019, V. 10, p. 73.

[11] Rastegaev I.A., Yasnikov I.S., Rastegaeva I.I., Agletdinov E.A., Merson D.L. Evaluating the probability of detecting acoustic emission signals using the amplitude discrimination method with a low signal-to-noise ratio. Russian journal of nondestructive testing, 2022, V. 58, pp. 157-166.

[12] Barat V., Borodin Y., Kuzmin A. Intelligent AE signal filtering methods. Journal of acoustic emission, 2010, V. 28, pp. 109-119.

[13] Altay Y.A., Fedorov A.V., Stepanova K.A. Acoustic emission signal processing based on polynomial filtering method. Proceedings of the IEEE conference Russian young researchers in electrical and electronic engineering. Saint Petersburg, Russia, 2022, pp. 1320-1326.

[14] Altay Y., Fedorov A.V., Stepanova K.A., Kuzivanov D.O. Estimating efficiency of acoustic emission signal processing methods in implementation of polynomial digital filters. *Omsk Nauchnyi zhurnal* [Omsk Scientific Bulletin]. 2022, no.3, pp. 128-134. (in Russian)

[15] Altay Y.A., Fedorov A.V., Stepanova K.A. Estimation of relationship between information components and noise of acoustic emission signals. *Kontrol. Diagnostica* [Testing. Diagnostics]. 2022, no. 7 (25), pp. 38-47. (in Russian)

[16] Barile, C., Casavola, C., Pappalettera, G., Vimalathithan, P. K.Acoustic emission descriptors for the mechanical behavior of selective laser melted samples: an innovative approach. Mechanics of materials, 2020, V. 148, pp. 103448.

[17] Selective laser melting (2024). Available at: https://www.sciencedirect.com/topics/materials-science/selective-laser-melting (accessed 15 January 2024)

[18] Direct laser growth (2024). Available at: http://www.ilwt-stu.ru/upload/publications/DMD_ru.pdf (accessed 15 January 2024)

[19] Fedorov A.V., Altay Y.A., Stepanova K.A., Kuzivanov D.O. The effect of signal-to-noise-ratio value on the error in measuring acoustic emission parameters: statistical assessment. Scientific and technical journal of information technologies, mechanics and optics, 2022, V. 22, pp. 1205-1215.

[20] Altay Y.A., Fedorov A.V., Stepanova K.A., Kuzivanov D.O. Acoustic emission signal filtering methods for identifying associations between diagnostic parameters of two milling cutter: experimental data. Proceedings of the 2022 IEEE international conference on electrical engineering and photonics. Saint Petersburg, Russia, 2022, pp. 1320-1326.

[21] Novikov A., Pronkin A., Vityazev S. Edge Detector Application in the Problem of Periodic Interference Filtering. Proceedings of the 2022 IEEE international conference on digital signal processing and its applications. Moscow, Russia, 2022, pp. 1320-1326.

[22] Tempelman, J. R., Wachtor, A.J., Flynn, E.B., Depond, P.J., Forien, J.B., Guss, G.M., Matthews, M.J. Detection of keyhole pore formations in laser powder-bed fusion using acoustic process monitoring measurements. Additive Manufacturing, 2022, V. 55, p. 102735.

[23] Pandiyan, V., Drissi-Daoudi, R., Shevchik, S., Masinelli, G., Le-Quang, T., Loge, R., Wasmer, K. Semi-supervised monitoring of laser powder bed fusion process based on acoustic emissions. Virtual and Physical Prototyping, 2021, V. 16, p. 481-497.

[24] Kuzivanov, D.O., Stepanova, K.A., Lobastov, M.M., Fedorov, A.V., Kinzhagulov, I.U. Analysis of Acoustic Emission Parameters During the Control of Samples at Their Direct Laser Melting. Proceedings of the IEEE 7th International conference on information, control, and communication technologies. Astrakhan, Russia, 2023, pp. 1-3.

[25] Altay Y.A. Improving the efficiency of noise resistance processing of speech signal. Proceedings of the IEEE conference Russian young researchers in electrical and electronic engineering. Saint Petersburg, Russia, 2017, pp. 618-620.

[26] Altay Y.A., Kremlev A.S., Zimenko K.A. A New ECG Signal Processing Method Based on Wide-Band Notch Filter. Proceedings of the IEEE conference Russian young researchers in electrical and electronic engineering. Saint Petersburg, Russia, 2020, pp. 1464-1469.

[27] Makhutov, N.A., Ivanov, V.I., Sokolova, A.G., Vasil'ev, I.E., Chernov, D.V., Skvortsov, D.F., Bubnov, M.A. Monitoring Composite Fiber Failure Using Acoustic Emission System, Vibration Analyzer, and High-Speed Video Recording. Russian Journal of Nondestructive Testing, 2020, V. 56, pp. 960-970.

[28] Zhang, W., Jia, H., Gao, G., Cheng, X., Du, P., Xu, D. Backing layers on electroacoustic properties of the acoustic emission sensors. Applied Acoustics, 2019, V. 156, pp. 387-393.

Authorized licensed use limited to: Satbayev University. Downloaded on April 03,2026 at 09:50:27 UTC from IEEE Xplore. Restrictions apply.